10th International Conference on
"Technical and Physical Problems of Electrical Engineering"
7-8 September 2014
Institute of Physics, Azerbaijan National Academy of Sciences
Baku, Azerbaijan

ICTPE Conference
www.iotpe.com
ictpe@iotpe.com
ictpe0@gmail.com

ICTPE-2014	Number 1	Code 01POW07	Pages 1-6

An Improved Dual Boost Converter with Zero Voltage Transition

H. Donuk [1] I. Iskender [2] N. Genc [3]

1. *Electrical Engineering Department, Sirnak University of Sirnak, Sirnak, Turkey,* hakan.donuk@gmail.com
2. *Electrical Electronics Engineering Department, Gazi University, Ankara, Turkey,* iresis@gazi.edu.tr
3. *Electrical Electronics Engineering Department, Yüzüncüyıl University, Van, Turkey,* nacigenc@gmail.com

Abstract- This work proposes a soft switching approach for dual-boost converter using an auxiliary resonant circuit. The topology is composed of a general dual-boost converter and an auxiliary resonant circuit including one switch, inductor, capacitor and diode. The auxiliary resonant circuit helps the main switch to operate under ZVT and ZCS conditions. The auxiliary switch also operates at soft switching mode. Furthermore, the proposed circuit removes the voltage stress on the main and auxiliary switches. Under soft switching conditions the efficiency of the converter increases. The converter has various advantages compared with the conventional boost converters as higher boost rate with low duty cycle, lower voltage stress on components and higher efficiency.

Keywords: Zero Voltage Transition, Dual-Boost Converter, Boost Converter.

I. INTRODUCTION

DC-DC converters controlled by Pulse Width Modulation technique have a wide range of application areas. Operating the converter at high frequency decreases the converter volume and increases the power density of converter. However, increasing the operating frequency increases the switching losses and the Electromagnetic Interference (EMI) resulting reduction in efficiency of converter [1]. Basically, switching losses are composed of switching losses of switches due to overlapping of voltage and current, loss of diodes due to reverse recovery phenomenon and discharge loss of the parasitic capacitor [2].

To reduce the switching losses several suppressing cells are made as RC/RCD, polar/non-polar, resonance/non-resonant and active/passive cells. The switching losses are greatly reduced by zero voltage switching method (ZVS) and the zero current switching (ZCS) method.

There have been published many papers about boost converter with active soft-switching methods. Boost type converter switching at zero voltage (ZVT) is one of the soft switching techniques given in [3].

There are methods given in [3], [4] and [5] in which the snubber cells cannot eliminate all the switching losses.

In [5-7] there are used multiple inductors that increase the volume and decrease the power density of the converter.

Soft switching techniques used in [6] and [8] reduces the losses but cannot remove the voltage stress of main and auxiliary switches.

The turn on and turn off losses are reduced in [9], but due to several numbers of elements the volume of the converter increases.

In another study [10] there are used more than one switch that increases the cost of the converter [10].

In the study given in [11] the active snubber circuit provides zero voltage transition modes for the main switch. There is no voltage and current stress on the main diode.

This work proposes a soft switching dual-boost converter that is able to turn on both the active power switches at zero voltages to reduce their switching losses and evidently raise the conversion efficiency. In this study dual-boost converter circuit is operating under soft switching technique and the efficiency of the converter increases by reducing the switching losses. The problem of voltage stress is also eliminated. The operation principles of the converter and the conditions for realization of soft switching are analyzed in detail, simulation analysis performed using PSpice is given. The simulation results show that all the switches are operating at soft switching state and the efficiency of the converter is improved.

II. CIRCUIT CONFIGRATION

Figure 1 represents the circuit configuration of the proposed dual-boost pulse-width modulation (PWM) converter.

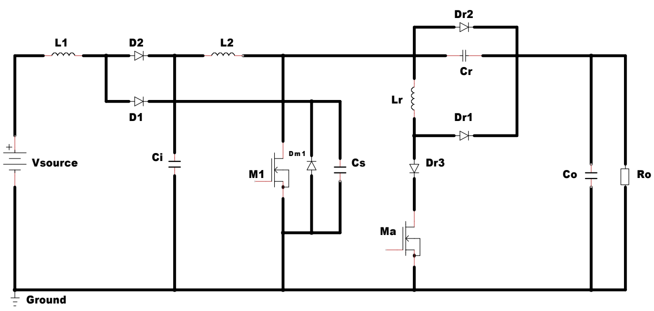

Figure 1. Proposed soft switched dual-boost DC/DC converter

The converter consists of one switch; two boost inductors L_1 and L_2; two diodes D_1 and D_2; and capacitors C_i and C_o. Except the output capacitance of the converter, the other components of the converter constitute the auxiliary circuit. M_a, D_{r1}, D_{r2}, and Dr_3 represent the auxiliary switch and diodes, respectively. The inductor and capacitor of proposed auxiliary circuit are presented by L_r and C_r, respectively. D_{m1} is the intrinsic parallel diode of MOSFET M_1 and the snubber capacitance, C_s is common for the main switch M_1.

III. CIRCUIT OPERATION ANALYSIS

The following assumptions are made in analysis of the converter.

- The output capacitor C_o is large enough to neglect reasonably the output voltage ripple and consider a constant level output voltage.
- The forward voltage drops on MOSFET M_1, M_a and diodes D_1 and D_2 are neglected.
- Inductors L_1 and L_2 are large and equal.
- The components of the converter are ideal.

The active switch, M_1 is operated with pulse-width-modulation (PWM) control signals. This is gated with identical frequency and duty ratio. The operation of the converter can be divided into seven modes, the equivalent circuits and the theoretical waveforms are illustrated in Figures 2 and 3.

A. Mode 1

Prior to this mode, the main switch M_1 and the auxiliary switch M_a are in the off state and output diode D_{r2} is conducting. At the beginning of this mode, M_a is turned on. The resonant inductor (L_r) current starts to rise through the path of V_{source}-L_1-L_2-L_r-M_a. Since the rise rate of this current is limited by L_r, the devices D_1 and M_a are turned on under soft switching. The voltage across C_s is nearly equal to the output voltage (V_o) in this interval and the initial voltage across the C_r is nearly equal to zero. During this time interval, the voltage across C_r and current of L_r can be expressed as: $t_0 < t < t_1$

$$\dot{I}_{Lr}(t) = \frac{Vcs}{Lr}(t_1 - t_0) = \frac{Vo}{Lr}(t - t_0) \quad (1)$$

$$V_{Cr}(t) = 0 \quad (2)$$

$$(t_1 - t_0) = \Delta t_1 = \frac{\dot{I}L1 * Lr}{Vo} \quad (3)$$

$$I_o(t) = I_{L1} - I_{Ci} - I_{Lr} \quad (4)$$

B. Mode 2

M_a current reaches i_{L1} and output current falls to zero at $t=t_1$. The snuber capacitor (C_s) begins to discharge and the current in L_r increases because of the resonance between L_r and C_s. C_s is discharged until its voltage reaches zero at t_2. The resonant time period of this interval, the current of L_r and voltage across C_s are given by; $t_1 < t < t_2$

$$I_{Lr}(t) = i_{L1} + \frac{Vo}{Z1} * \sin \omega_1 (t - t_1) \quad (5)$$

$$V_{Cs}(t) = V_o \cos \omega_1 (t - t_1) \quad (6)$$

$$(t_2 - t_1) = \Delta t_2 = \frac{\pi}{2}\sqrt{LrCs} \quad (7)$$

$\omega_1 = 1/\sqrt{LrCs}$ and $Z = \sqrt{LrCs}$

C. Mode 3

At $t=t_2$, the main switch and D_2 are in the off state and auxiliary switch and D_1 are in the on state. Auxiliary switch conducts the current in L_r. At the beginning of this mode current of snubber capacitor C_s is completely exhausted and the L_r current reaches its maximum rate.

At this interval, the current in L_r flows in L_r- M_a and body diodes of the main switches. The voltage across C_r is discharged nearly to zero before t_2. The maximum current of L_r can be equated as;

$$\dot{I}_{Lr}(t) = I_{Lrmax} = I_{L1} + V_o / Z_1 \quad (8)$$

$$V_{Cr}(t) \cong 0 \quad (9)$$

At this mode, the main switch should be switched to satisfy the ZVT condition. By assuming the average inductor current of L_1 is the half of the input current at steady state, the delay time for M_1, t_d can be expressed as;

$$t_d = \Delta t_1 + \Delta t_2 = \frac{Iin * Lr}{Vo} + \frac{\pi}{2}\sqrt{LrCs} \quad (10)$$

Additionally, the current through inductors will start to increase linearly according to;

$$I_{L1} = \frac{Vs}{L1 + Lr}(t_3 - t_2) \cong \frac{Vs}{L1}(t_3 - t_2) \quad (11)$$

$$I_{L2} = \frac{VCi}{L2 + Lr}\, t \cong \frac{VCi}{L2}\, t \quad (12)$$

D. Mode 4

At the start of this interval, M_a is turned off and the main switch is turned on at the same time. At this mode, the main switche, M_1 and L_r conduct the input current together. At the end of this mode the current of L_r and L_1, L_2 reaches zero.

$$I_{L1} = \frac{Vs - Vo}{L1 + Lr}(t_4 - t_3) \cong \frac{Vs}{L1}(t_4 - t_3) \quad (13)$$

$$I_{L2} \cong \frac{Vci}{L2}(t_6 - t_4) \quad (14)$$

E. Mode 5

This interval is composed of two equivalent circuit. The energy is stored in the boosting inductor L_1 through the loop of V_{source}-L_1-D_1-M_1 and stored in the boosting inductor L_2 through the loop of C_i-L_2-M_1. The energy is transferred to the load through discharging capacitor, C_o. The current of L_1;

$$I_{L1} = \frac{Vs}{L1}(t_5 - t_4) \quad (15)$$

F. Mode 6

At t_5, the current of main switch falls to zero and voltage across of M_1 and C_s go up to output voltage V_o. At the end of this interval the current of L_r starts to increase.

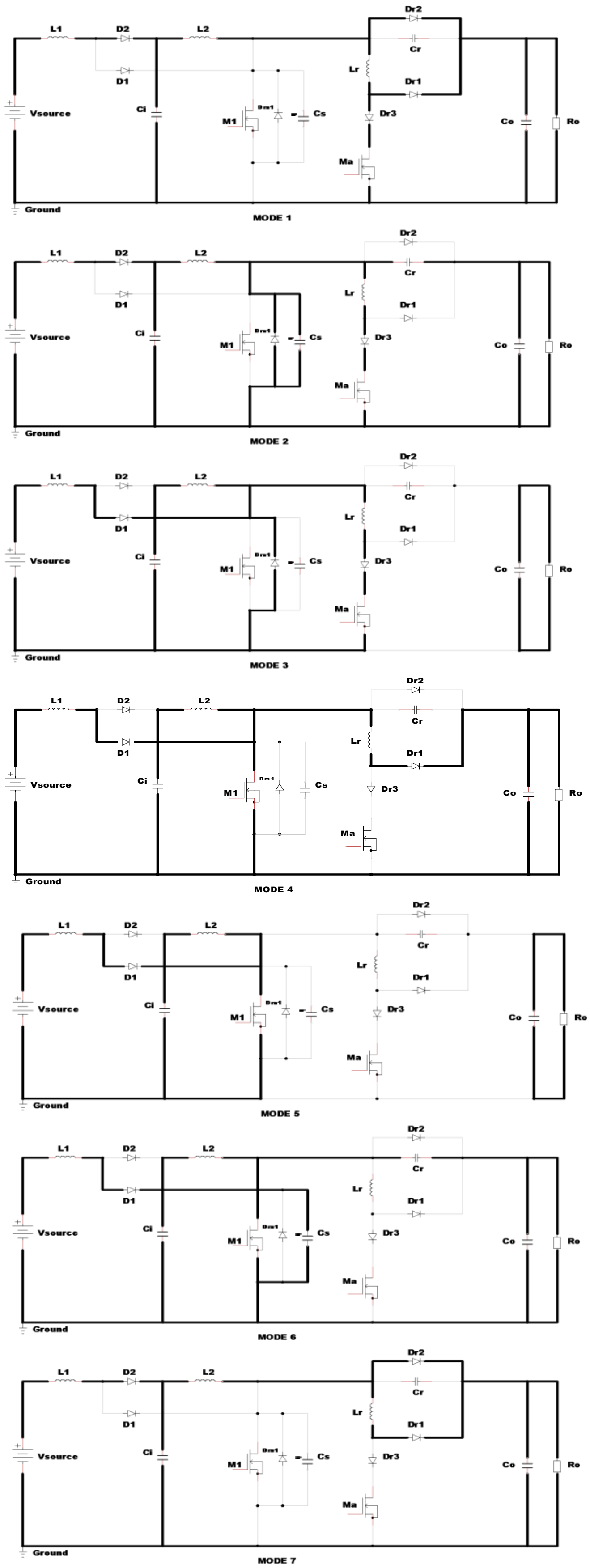

Figure 2. Operational modes of proposed circuit converter.

G. Mode 7

At a certain moment t_6, D_2 and main switch are turned off. D_2, D_{r1} and D_{r2} are turned on. The inductor currents I_{L1} and I_{L2} at the that moment have reached peak values. The stored energy is supplied to load through diodes D_2, D_{r1} and D_{r2}. As a result, the current through the inductors I_{L1} and I_{L2} will start to decrease linearly according to;

$$I_{L1} = \frac{Vs - Vci}{L1}(t_6 - t_7) \quad (16)$$

$$I_{L2} = \frac{Vci - Vo}{L2 + Lr}(t_6 - t_7) \quad (17)$$

Current C_i is inversed again, and C_i is now charging until D_1 is turned on again and the cycle with its seven intervals is repeated.

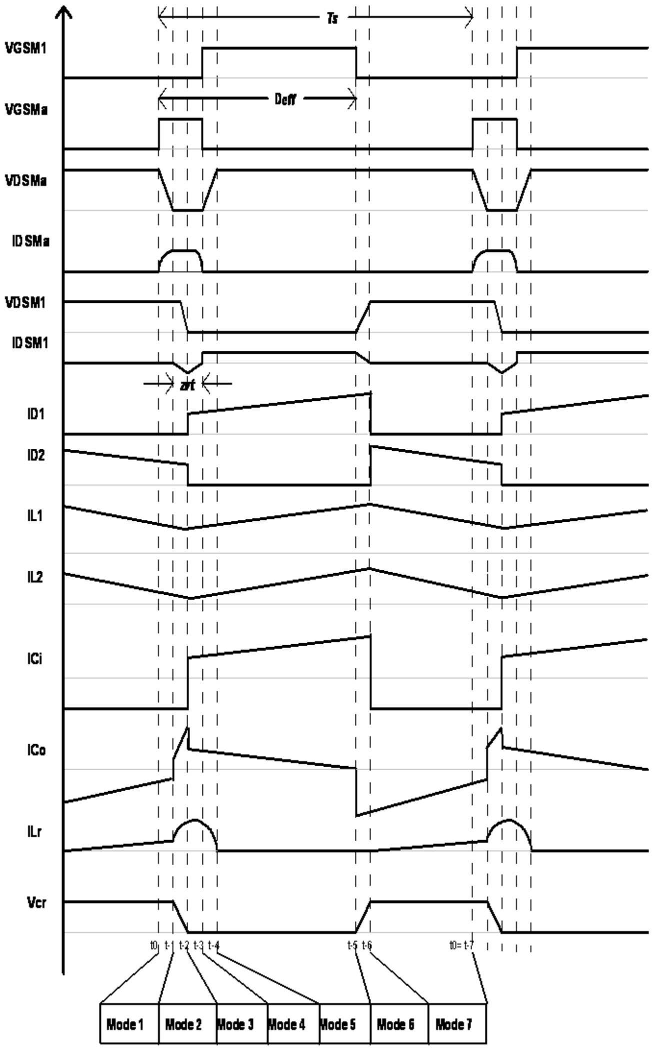

Figure3. Theoretical waveforms of the proposed circuit topology.

IV. CİRCUIT DESIGN AND SELECTION OF COMPONENTS

The boost converter is a high-efficiency step-up DC/DC switching converter. The converter uses a switch to transfer power through pulse-width modulation technique. This section presents a design procedure for the proposed soft switched dual-boost converter operating in continuous conduction mode (CCM). In the periodic switching scheme with period *T*, the average voltage across the inductor must be zero. The relationship of voltage and current for an inductor is

$$V_L = L\frac{diL}{dt}, \quad (18)$$

$$\dot{I}_L(t) = \frac{1}{L}\int_0^t VL(t)\,dt + \dot{I}_L(0), \quad (19)$$

$$\dot{I}_L(t) = \frac{1}{L}\int_{t0}^t VL(t)\,dt + \dot{I}_L(t_o), \quad (20)$$

$$\dot{I}_L(T+t_o) = \frac{1}{L}\int_{t0}^{T+t} VL(t)\,dt + \dot{I}_L(t_o), \quad (21)$$

$$\dot{I}_L(T+t_o) - \dot{I}_L(t_o) = \frac{1}{L}\int_{t0}^{T+t} VL(t)\,dt\,. \quad (22)$$

$$i(t)=i(t+T), \quad t=t_o, \text{ and } V_L = \frac{1}{L}\int_{t0}^{T+t} VL(t)\,dt = 0$$

According to the voltage second product,

$$V_s * t_{on} = (V_{Ci} - V_s) * t_{off} \text{ or } V_s T = V_{Ci} * t_{off} \quad (23)$$

$$V_{Ci} = \frac{T}{toff} V_s = \frac{T}{T-ton} V_s \quad (24)$$

$$V_{Ci} = \frac{1}{1-(Daux+Dmain)} V_s, \quad (25)$$

$$D_{eff} = D_{aux} + D_{main}$$

D_{main} is duty cycle of the main switch and D_{aux} is the duty cycleof the auxiliary switch. The same procedure is used to find the relation between the output voltage V_o and the first stage output V_{Ci}:

$$V_{Ci}\; t_{on} = (V_o - V_{Ci})\, t_{off}, \quad (26)$$

$$V_{Ci}\; (t_{on} + t_{off}) = V_o\, t_{off}, \quad (27)$$

$$V_o = \frac{T}{toff} V_{Ci} = \frac{T}{T-ton} V_{Ci}, \quad (28)$$

$$V_o \cong \frac{1}{1-(Daux+Dmain)} V_{Ci} \cong \frac{1}{1-Deff} V_{Ci} \quad (29)$$

$$V_o = \frac{1}{1-Deff} V_{Ci} = \frac{1}{(1-Deff)\,2.} V_s \quad (30)$$

The gain of the dual-boost DC-DC converter will be

$$V_o \cong \frac{1}{(1-Deff)\,2.} V_s\;. \quad (31)$$

To achive the zero voltage transition, a delay time (T_{delay}) of main switch PWM is required. The minimum delay time must be satisfied the following equation. The time is consisted of the resonant time between L_r and C_s and the time that the resonant inductor current equals the input current.

$$T_d \geq \frac{Iin*Lr}{Vo} + \frac{\pi}{2}\sqrt{LrCs} \quad (32)$$

It is seen from equation (32) that T_d depends on V_o, I_{in}, L_r and C_s. During the delay time, the auxiliary switch is turned on.

The input current ripple ΔI_L on each of the boost inductors can be denoted as:

$$\Delta I_L \cong \Delta I_{L1} = \frac{Deff}{L1*f} V_s, \quad (33)$$

An ideal output capacitor the output voltage ripple can be determined as:

$$\Delta Vo = \frac{Io*Deff}{C*f}, \quad (34)$$

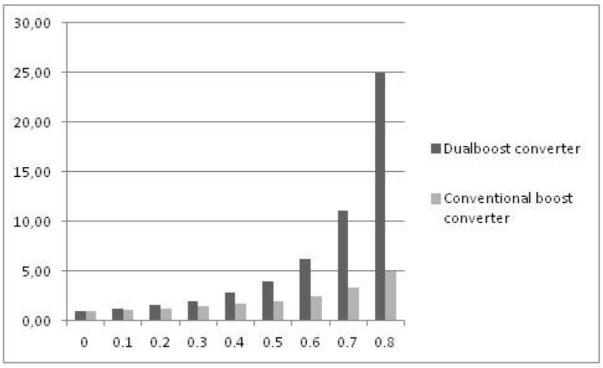

Figure 4. Voltage conversion ratio.

V. SIMULATION

In this section, simulations are carried out to verify the theoretical analysis given in the previous sections. Since the PSpice simulation program includes models of the real components, the proposed topology is firstly simulated via this program and the simulation results of the proposed topology are shown in the following figures. The converter design specifications are considered for medium power sources. Since the output voltage generated by the photovoltaic arrays and the fuel stack sources is relatively low, their output voltage is generally increased via conventional boost or dual-boost type dc-dc converters to the required voltage level. The converter specifications consist of,

Output power: P_o =600 W,
Output voltage ripple, ΔVo= %2,
Input current ripple, ΔI_L = %15,
Switching frequency: f_s = 50 kHz,

Table 1. Components values for the simulation

Components	Symbols	Parameters
Input voltage	V_{source}	100 V
Output voltage	V_{output}	300 V
Switching frequency	f_{sw}	50 kHz
Main inductances	L_1 and L_2	300 uH
Auxiliary inductance	L_r	1 uH
Auxiliary capacitance	Cr	5 nF
Snubber capacitance	C_s	1 nF
Input capacitance	C_i	30 uF
Output capacitance	C_o	50 uF
Main switch	M_1	IRF250-30A
Auxiliary switch	M_a	IRF350-14A
Main diodes	D_1 and D_2	MUR810
Auxiliary diodes	D_{r1} ,D_{r2}, D_{r3} and D_m	MUR810
Output power	P_o	600 W

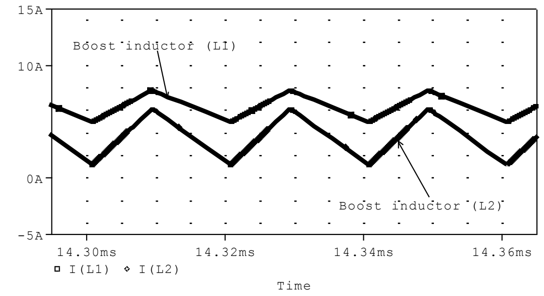

Figure 5. Simulation waveforms of the current of the inductors (I_{L1} and I_{L2})

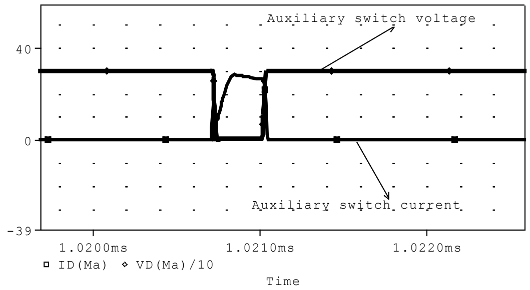

Figure 6. Simulation waveforms of the voltage and current of the auxiliary switch M_a (V_{DMa}/10, I_{DMa} and P_o= 600 W- V_o = 300 V)

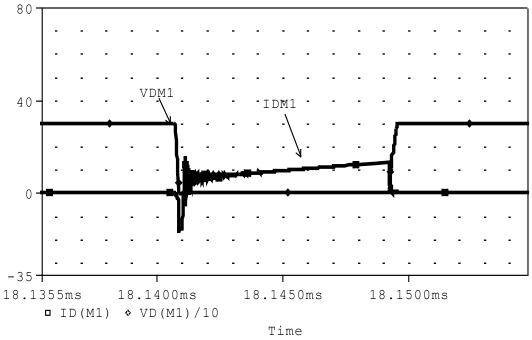

Figure 7. Simulation waveforms of the voltage and current of the main switch M_1 (V_D/10, I_{DM1}) under soft switching condition.(P_o= 600 W- V_o = 300 V)

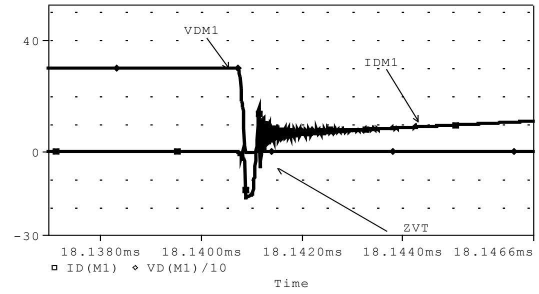

Figure 8. Simulation waveforms of the voltage and current of the main switch M_1 (V_D/10, I_{DM1}) under soft switching condition turn on. (P_o= 600 W- V_o = 300 V)

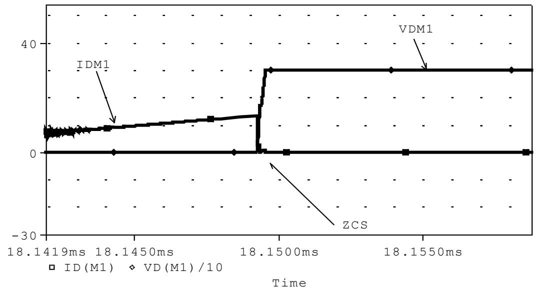

Figure 9. Simulation waveforms of the voltage and current of the main switch M_1 (V_{DM1}, I_{DM1}) under soft switching condition turn off (P_o= 600 W- V_o = 300 V)

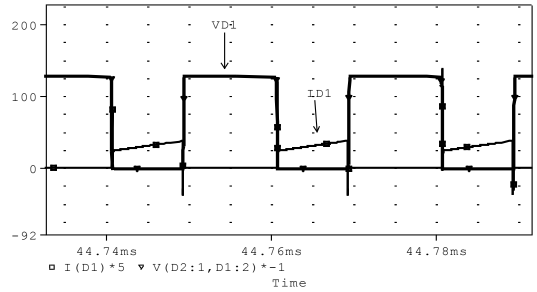

Figure 10. Simulation waveforms of the voltage and current of the main diode D1 (V_{D1} , I_{D1} *5) under soft switching condition (P_o= 600 W- V_o = 300 V)

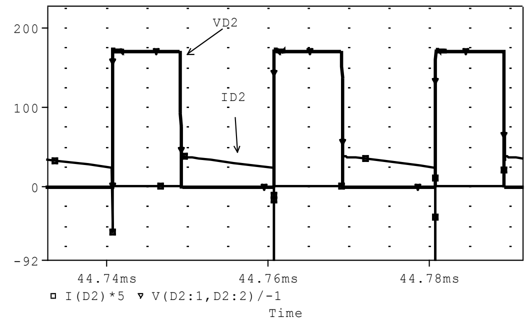

Figure 11. Simulation waveforms of the voltage and current of the main diode D2 (V_{D2} , I_{D2} *5) under soft switching condition (P_o= 600 W- V_o = 300 V)

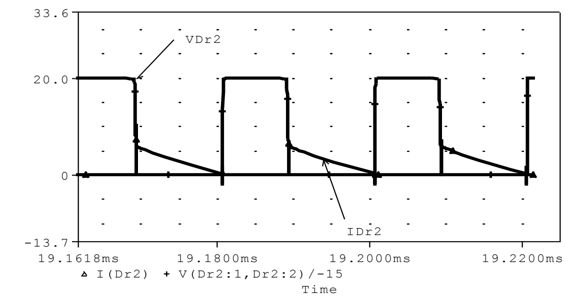

Figure 12. Simulation waveforms of the voltage and current of the auxiliary diode Dr2 (V_{Dr2}/15, I_{Dr2}) under soft switching condition (P_o= 600 W- V_o = 300 V)

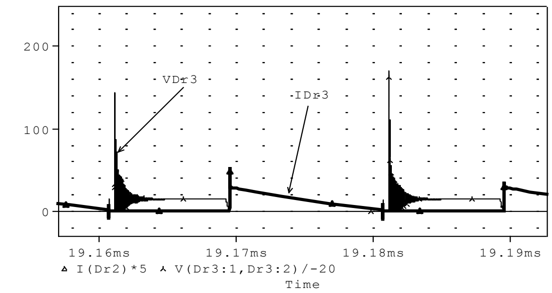

Figure 13. Simulation waveforms of the voltage and current of the auxiliary diode Dr3 (V_{Dr3}/20, I_{Dr3} *5) under soft switching condition (P_o= 600 W- V_o = 300 V)

From the simulation results given in figures 12 and 13, it is seen that the main switch M_1 is turned on perfectly with ZVT and turned off under near ZCS. Figure 9 shows auxiliary switch, M_a which is turned on and off under soft switching. Also, the devices D_1, D_2, D_{r1}, D_{r2} and D_{r3} operate under soft switching conditions. The losses of the semiconductor devices and the total efficiencies of the circuits for hard switching and the proposed soft switching cases are summarized for various loads as given in Table 2.

Table 2. Losses of the semiconductor devices and total efficiencies of the circuits in the hard switching and the proposed soft switching converter

Vsource: 100 V, Vo: 300 , Freq: 50 kHz							
DC-DC DUALBOOST CONVERTER							
LOAD %	HARD OR SOFT	POWER LOSSES			INPUT POWER	OUTPUT POWER	EFFİCİENCY %
		MAİN SWİTCH	AUXILIARY SWİTCH	DİODES AND OTHER			
20	HARD	3,3	NONE	7,3	130,6	120	91,80
	SOFT	1,1	1,95	8,0	11,1	120	91,50
25	HARD	4,0	NONE	5,4	159,4	150	94,10
	SOFT	1,0	2	5,8	161,6	150	92,80
50	HARD	7,6	NONE	7,8	315,4	300	95,10
	SOFT	3,4	4,7	9,0	317,1	300	94,60
75	HARD	13,2	NONE	9,1	472,3	450	95,20
	SOFT	5,4	8,1	6,5	470,0	450	95,75
100	HARD	20,3	NONE	10,8	631,1	600	95,00
	SOFT	9,2	9,27	8,3	626,7	600	95,70

At 450 W output power in the hard switching operation the main switch loss is about 13,2 W and this loss is equal %59,1 of total loss of circuit. At 450 W output power in the proposed soft switching converter, the main switch loss is about 5,4 W and this loss is equal %27 of total loss of circuit.

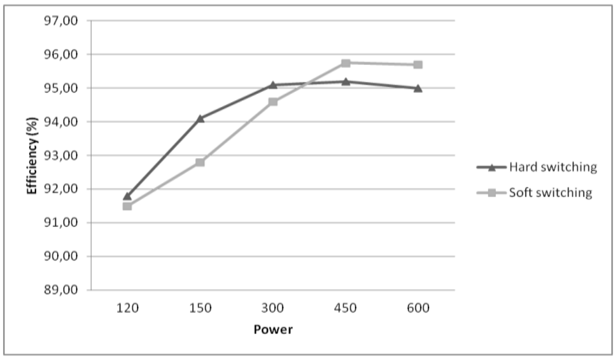

Figure 14. Overall efficiency curves of the hard switching and the proposed soft switching converters comparatively

VI. CONCLUSION

In this paper, a soft switching dual-boost converter using an auxiliary resonant circuit is proposed. Operation modes are divided considering the voltage and current waveforms. Equivalent circuit of each operation mode is illustrated and the current paths are indicated. Each mode is analyzed through the simulation. It is verified that the main switch operates at soft switching. The main switch is turned on with ZVT and turned off under near ZCS. The auxiliary switch turned on and turned off under the soft switching mode. In addition, the main diodes and auxiliary diodes turn on and off under soft switching cases. It can be clearly seen that the predicted operation principles and analysis of the proposed converter are verified with all of the simulation results. In the proposed converter, most of the drawbacks of the conventional ZVT converter are overcome both perfectly and easily. All the semiconductor devices of the converter are both turned on and off under soft switching state. There is no any additional voltage and current stresses on the main devices and the auxiliary devices.

NOMENCLATURES

ΔI_L : *Input current ripple*
ΔVo: *Output voltage ripple*
Z : Impedance of the auxiliary circuit
D_{eff} : *Effective duty cycle rate*

....

REFERENCES

[1] Huang, W. ve Moschopoulos, G., (2006). " A New Family of Zero-Voltage-Transition PWM Converters with Dual Active Auxiliary Circuits", Power Electrons, IEEE Transactions on, 21: 370-379
[2] Aksoy, İ., (2007). Yeni Bir Yumuşak Anahtarlamalı DC-DC PWM Dönüştürücünün Tasarımı, Analizi ve Uygulaması, Doktora Tezi, YTÜ Fen Bilimleri Enstitüsü, İstanbul.
[3] G. Hua, C. Leu, Y. Jiang and F. Lee " Novel Zero-Voltage-Transition PWM Converters", IEEE Transaction on Power Electronics, 9(2): 213-219 (1994).
[4] H. Bodur, A. F. Bakan "A new ZVT-PWM DC-DC Converter" IEEE Transaction on Power Electronics, 17(1): 40-47 (2002).
[5] M. Phattanasak, "A ZVT Boost Converter using an Auxiliry Resonant Circuit" Power Electronics, Drives and

Energy Systems, 2006. PEDES'06 International Conference on,pp.1-6,12-15 Dec. 2006
[6] A.F. , Bakan, H., Bodur, and I., Aksoy, "A Novel ZVT-ZCT-PWM DC-DC Converter", 11th Europen Conference on Power Electronics and Applications (EPE2005), Dresden, pp.1-8,Sept.2005
[7] R. Gurunathan and A.K.Bhat ,"ZVT boost converter using a ZCS auxiliary circuit, " IEEE Trans. Aerosp. Electron. Syst.,vol. 37, no.3 ,pp.889-897,Jul.2001
[8] Iskender, I., & Genc, N. (2010). "Design and analysis of a novel zero-voltage-transitions interleaved boost converter for renewable power applications." International Journal of Electronics, 97, 1051-1070. doi: 10.1080/00207217.2010.482021
[9] Jain, N., Jain, P., and Joos, G.(2001) " Analysis of a zero voltage transition boost converter using a soft switching auxiliary circuit with reduced condition losses " in IEEE PESC Conference Record, Vol. 4,2001 , 1799-1804.
[10] Gurunathan, R. and Bhat, A. K. S.," A zero-voltage-transition boost converter using a zero voltage switching auxiliary circuit", IEEE Transactions on Power Electronics, 17:658-668 (2002).
[11] Bodur, H. and Bakan, A.F., (2004). "A New ZVT–ZCT–PWM DC–DC Converter", IEEE Trans. On Power Electron, 19(3): 676-684.
[12] Khairy, S., Mazen, A., Adel, A., and Mahmoud, A.,"New High Voltage Gain Dual-boost DC-DC Converter for Photovoltaic Power Systems", Electric Power Components and Systems, 40:711-728, 2012
……………………………………………………….

BIOGRAPHIES

Hakan Donuk was born in Diyarbakir, Turkey, 1987. He received the B.Sc. degree in Electric and Electrical Engineering from Dicle University, Diyarbakir, Turkey and is currently working on his MS thesis in Gazi University. His research areas include soft switching, active-passive snubber cells in power electronics, renewable energy.

Ires Iskender received his M.Sc. and Ph.D. degrees in Electrical and Electronic Engineering in 1990, 1996, respectively, from Middle East Technical University, Turkey. He is currently an Professor in the Department of Electrical and Electronic Engineering, Gazi University, Ankara, Turkey. His research interests include power electronic, renewable energy, fuzzy control, electrical machine, power quality

Naci Genc completed his B.S. in Electrical Education Department from Gazi University, Ankara. He received his MS from Electrical & Electronics Engineering Department of Yuzuncu Yil University and Ph.D. Degrees from Electrical & Electronics Engineering Department of Gazi University in 2002 and 2010, respectively. From 1999 to 2010 he worked as a research assistant in the Electrical and Electronics Engineering Department of Yuzuncu Yil University, Middle East Technical University and Gazi University, Turkey. He is currently an Associate Professor at Yuzuncu Yil University, Van. His research interests include power electronics, electrical machines, renewable energy, solar photovoltaic energy systems and control systems.